HHS Public Access

Author manuscript

Exp Gerontol. Author manuscript; available in PMC 2021 August 28.

Published in final edited form as:

Exp Gerontol. ; 134: 110893. doi:10.1016/j.exger.2020.110893.

MANF delivery improves retinal homeostasis and cell replacement therapies in ageing mice

Joana Neves[1,2,*], **Kathleen R. Chirco**[3,5], **Wendy Cedron-Craft**[1,5], **Shereen Chew**[3], **Jie Zhu**[1], **Heinrich Jasper**[1,4], **Deepak A. Lamba**[1,3,*]

[1]Paul F. Glenn Center for Biology of Aging Research, Buck Institute for Research on Aging, 8001 Redwood Boulevard, Novato, CA 94945-1400, USA

[2]Instituto de Medicina Molecular (iMM), Faculdade de Medicina, Universidade de Lisboa, Lisbon, 1649-028, Portugal

[3]The Eli and Edythe Broad Center of Regeneration Medicine and Stem Cell Research, Department of Ophthalmology, University of California, San Francisco, San Francisco, USA

[4]Immunology Discovery, Genentech, Inc., 1 DNA Way, South San Francisco, California 94080, USA.

[5]Equal contribution

Abstract

Ageing is a major risk factor for vision loss, and inflammation is an important contributor to retinal disease in the elderly. Regenerative medicine based on cell replacement strategies has emerged in recent years as a promising approach to restore vision. However, how the ageing process affects retinal homeostasis and inflammation in the retina and how this may impose a limitation to the success of such interventions remains unknown. Here we report that, in mice and humans, retinal ageing is associated with a reduction in MANF protein levels, specifically in the choroid, where increased densities of activated macrophages can be detected. We further show that the retina of old wild type mice, in the absence of any other genetic alteration, has limited homeostatic capacity after damage imposed by light exposure and reduced engraftment efficiency of exogenously supplied photoreceptors. Finally, we show that supplementation of MANF recombinant protein can improve retinal homeostasis and repair capacity in both settings, correlating with reduced numbers of activated macrophages in the old retina. Our work identifies age-related alterations in retinal homeostasis, independent of genetic alterations, leading to age-

*Correspondence to: J.N., joana.neves@medicina.ulisboa.pt; D.A.L., Deepak.Lamba@ucsf.edu.

Author Contributions

JN, HJ and DAL conceived the study. JN designed and performed experiments in mice, collected and analyzed the data. WCC, SC and JZ performed experiments in mice and collected data. KC conceived and performed the analysis of human tissue and analyzed and interpreted the data with input from DAL. JN interpreted the data and wrote the manuscript with input from HJ and DAL. All authors revised the manuscript.

Data Availability Statement

The data that support the findings of this study are openly available in zenodo at https://doi.org/10.5281/zenodo.3443779

related retinal inflammation and damage susceptibility. We suggest that MANF therapy is a potential intervention to maintain retinal homeostasis in the elderly and improve the success of retinal regenerative therapies applied to aged individuals.

Introduction

Age-related macular degeneration (AMD) defines the progressive degeneration of the macula, leading to vision impairment in over 30 million people worldwide, and is commonly observed after 60 years of age (AMD Alliance International, 2010). Despite its multifactorial nature and the identification of multiple genetic variants associated with risk of developing AMD, ageing stands alone as the single most important risk factor for the disease (Ardeljan and Chan, 2013), suggesting that biological alterations naturally associated with the ageing process are likely contributors to disease progression. Age-related alterations in immune pathways and the consequent dysregulation of the inflammatory response are considered central players in AMD (Ambati et al., 2013), and a common feature of many ocular diseases (Perez and Caspi, 2015). Further highlighting the importance of inflammatory mechanisms in AMD, therapies currently being evaluated in clinical trials to treat or prevent the consequences of the disease are based on the modulation of immune mechanisms (Ambati et al., 2013). Alternatively, stem-cell based regenerative therapies, in which replacement cells are used to repair the damaged retina, have also been extensively validated in pre-clinical settings as means to restore vision (Lamba et al., 2009; MacLaren et al., 2006) and have been positively evaluated in a clinical trial (Mandai et al., 2017). Importantly, the success of cell replacement therapies in animal models also depends on the optimal management of inflammatory pathways (Neves et al., 2016; West et al., 2010). Thus, it is likely that in elderly patients, who may benefit from these therapies, the inflammatory condition associated with ageing will also impose important roadblocks to the success of stem-cell based regenerative therapies for the treatment of AMD (Neves et al., 2017).

Like many age-related diseases, AMD is associated with a loss of tissue (retinal) homeostasis, and it has been proposed that age-related changes create susceptibility for the development of a pathological condition. In the case of AMD, it has been proposed that defective immune responses limit tissue repair capacity and result in accumulation of tissue damage, causing a subsequent hyperactivation of the immune system that further contributes to disease progression (Ambati et al., 2013; Ardeljan and Chan, 2013). Thus, intervening at early stages of AMD likely requires immune modulatory strategies that restore an effective repair-associated immune response. This type of approach may also be beneficial in combination with stem-cell based repair therapies, where deficient repair capacity of aged tissues may impose a limitation to regenerative success (Neves et al., 2017).

Despite the central role of age-related alterations in the development of AMD, most of the research so far has been focused on generating animal models with specific genetic defects in pathways that can recapitulate genetic variants observed in patients. However, knowledge on the specific contribution of physiological ageing alterations, including age-related inflammation, for the loss of retinal homeostasis is still limited. We recently identified Mesencephalic Astrocyte-derived Neurotrophic factor (MANF) as an evolutionarily-

conserved regulator of immune homeostasis during ageing (Sousa-Victor et al., 2019). MANF levels decline with age, in tissues and in circulation, in flies, mice and humans. Loss of MANF results in a phenotype of sterile inflammation at middle age with accumulation of activated macrophages in several tissues. Restoring MANF levels in old mice is sufficient to reestablish immune homeostasis and limit tissue damage, at least in the liver (Sousa-Victor et al., 2019). We have further shown that the immune modulatory function of MANF can be harnessed to promote repair capacity in the young retina, limiting photoreceptor damage and promoting functional retinal repair and vision recovery following photoreceptor transplantation in young mice (Neves et al., 2016). However, the limitations in tissue repair of the aged retina have not yet been evaluated, nor has the utility of MANF and immune modulatory interventions applied to the aged retina.

Results

To gain further insight into the specific changes that occur in the aged retina, we analyzed ocular tissue from young (yg, 3-4 months) and old (20-24 months) C57BL6/NJ wild type (wt) mice. Gene expression analysis, based on RT-qPCR quantification of transcript abundance in whole-eye RNA extracts, revealed a significant reduction of MANF levels (Fig. 1a). Age-associated reduction in MANF was associated with inflammatory phenotypes in other tissues (Sousa-Victor et al., 2019). In ocular tissue we observed a significant reduction in Cx3cl1 expression levels and concomitant increase in Ccl2 levels (Fig. 1a), in agreement with previous studies (Chen et al., 2010; Sennlaub et al., 2013). Considering that the corresponding receptors of these ligands, Cx3cr1 and Ccr2, define two distinct populations of monocytes with antiinflammatory and pro-inflammatory profiles, respectively (Geissmann et al., 2003), the results suggest an increased propensity of the old retina to recruit and/or accumulate inflammatory macrophages. Indeed, we found that ocular tissue from old mice consistently showed increased densities of activated (pro-inflammatory) macrophages, identified by CD68+ immune reactivity, when compared with the eyes of young mice (Fig. 1b and Supplemental Fig. S1). This is similar to what has been observed in early stages of AMD in humans (Cao et al., 2011).

Immunostaining of whole eye cryosections revealed MANF expression in different retinal cell types and in the choroid, as detailed in previous reports (Gao et al., 2017; Gao et al., 2016; Lu et al., 2018; Neves et al., 2016). While protein levels of MANF were not significantly different between young and old whole eye protein extracts, evaluated by ELISA (Supplemental Fig. S2a) and confirmed by quantification of whole eye immunostaining (Supplemental Fig. S2b), quantification of MANF immune reactivity in different anatomical locations within eye cryosections revealed a significant reduction in MANF protein levels in the choroid region specifically (Fig. 1c). Interestingly, the sites of increased densities of CD68+ cells corresponded to the anatomical locations in the eye where a significant reduction in MANF protein levels was observed (Fig. 1c-d): high magnification analysis of eye tissue sections showed that the CD68+ cells found in the eyes of old mice (Fig. 1b) were located in the choroid region (Fig. 1d). Co-staining with Iba-1, a pan-macrophage marker, revealed that these changes do not represent an increased density of macrophages, per se, in the choroid, but rather a decrease in the proportion of macrophages that express MANF (Supplemental Fig. S2c), and an increase in the proportion

of macrophages that express CD68 (Fig. 1e and Supplemental Fig. S2d), indicative of pro-inflammatory activation.

In other organs we observed a similar increase in the density of pro-inflammatory activated macrophages during ageing, that could be reproduced in middle aged mice with reduced MANF levels (MANF heterozygous - MANFHet mice), suggesting that MANF loss can be at least part of the mechanism leading to the phenotype of sterile inflammation (Sousa-Victor et al., 2019). To test if this mechanism also contributes to the phenotype observed in old eyes, we analyzed ocular tissue from middle aged MANFHet mice and found a significant increase in the densities of CD68+ macrophages in the choroid, when compared to age matched wt littermates, without affecting the total number of macrophages (Fig. 1f and Supplemental Fig. S2e). These observations mimic the phenotype observed in the choroid from aged animals and suggest that MANF loss is at least partly contributing to the increase in inflammatory macrophages in the choroid of old animals,

Age-related changes in MANF protein levels were also observed in human eyes: analysis of eye tissue from non-diseased donors aged 74 and 79 yrs., showed a reduction in MANF levels in the choroid region (Fig. 1g) when compared with the retinae of two young donors (non-diseased, aged 21 and 32 yrs.). Upon co-staining with IBA-1 to mark immune cells, colocalization between IBA-1 and MANF in the choroid (identified by UEA-1 staining) was observed with higher frequency in young control eyes when compared to aged controls (Fig. 1g, asterisks). IBA-1 + cells with lower levels of MANF protein were more frequent in the choroid of old donors (Fig. 1g, arrowheads). MANF levels in the neural retina were not changed and mainly detected in the ganglion cell layer (Supplemental Fig. S2f), in agreement with previous reports (Gao et al., 2016). Thus, we observed a choroid-specific decline in MANF levels in ocular tissue associated with the accumulation of activated pro-inflammatory macrophages in the same region.

Tissue inflammation compromises homeostasis. Thus, we asked whether the changes in the immune environment in old eyes were sufficient to limit retinal homeostatic capacity, defined as the ability to limit photoreceptor death after a damage stimulus. Using an experimental paradigm of light-induced acute retinal damage (Neves et al., 2016), we found a significant increase in the number of apoptotic photoreceptors in the retina of old mice, when compared to the retina of young mice, after light exposure (Fig. 2a-b). In the absence of light exposure there were very few apoptotic photoreceptors in the retina of both young and old mice (Fig. 2b).

Indeed, as previously reported by us and others, the young retina of C57BL6/J mice showed a robust homeostatic capacity in response to light damage that resulted in very little apoptosis of photoreceptors (Neves et al., 2016; Wenzel et al., 2001). While multiple mechanisms may contribute to this homeostatic capacity (Wenzel et al., 2001), MANF mediated signaling is involved: In the young retina, there is an endogenous repair mechanism involving MANFmediated immune modulation that limits tissue damage in response to light exposure (Neves et al., 2016). Consistently, mice with reduced MANF levels (MANFHet mice), unlike wt mice, exhibit significant apoptosis of photoreceptors when exposed to the same light dosage and MANF supplementation is sufficient to limit

photoreceptor apoptosis in young mice under different pathological conditions (Neves et al., 2016). Thus, we asked whether MANF supplementation would also be sufficient to limit tissue damage in the retina of aged mice. We found that one single intravitreal injection of human recombinant MANF protein (hrMANF) significantly reduced the number of apoptotic photoreceptors in the old retina after light exposure (Fig. 2a-b). Of note, this intervention provided supra-physiological levels of MANF and aimed not only overcome the age-related decline in MANF levels, but to provide a direct pro-repair signal that can limit tissue damage as observed in young mice (Neves et al., 2016).

In young mice, MANF limits photoreceptor apoptosis by modulating phenotypes of macrophages that invade the retina during the tissue damage response. (Neves et al., 2016). Since infiltration of pro-inflammatory macrophages precedes retinal degeneration in experimental models of AMD (Cruz-Guilloty et al., 2013), and has been deemed causal to photoreceptor loss in other models of retinal degeneration (Peng et al., 2014), we asked whether the reduction in photoreceptor apoptosis elicited by MANF in old mice was accompanied by modulation of immune infiltrates in the photoreceptor layer. We observed a significant increase in the number of activated macrophages within the outer nuclear layer (ONL) of old mice when compared to young mice after light exposure, suggesting that the choroid population may invade the retina in damage conditions. Importantly, MANF treatment also significantly reduced the number of CD68+ macrophages in the ONL of light-exposed retinae (Fig. 2c), mimicking the effects of systemic treatment of MANF in other organs (Sousa-Victor et al., 2019). This opens the possibility that, as in young mice, MANF effects in the old retina could also be dependent on immune modulation (Neves et al., 2016). It further suggests that the pro-repair function of MANF can be harnessed to limit tissue damage in the old retina, potentially reducing the risk of retinal degeneration in response to external stress.

One of the major targets of regenerative therapies is ageing individuals with diseases including AMD. We hypothesized that the aged immune environment may also be a limitation to regenerative success in old retinae (Neves et al., 2017). To test this idea, we performed subretinal transplants of Nrl-GFP+ photoreceptors isolated from P6 animals into the eyes of young (2-4 mo) and old (24-30 mo) wt mice and evaluated the number of GFP+ cells in the ONL 14 days after transplant. We found that ageing alone, in the absence of other defects, imposes important limitations to the success of this intervention: the number of GFP+ cells found in the ONL of retinae from old mice that received transplants was significantly lower than in young mice (Fig. 3a-b). In young mice, inflammatory environments correlate with sites of poor repair (evaluated by GFP+ cells in the ONL, (West et al., 2010)) and MANF supplementation is sufficient to improve repair capacity in young mouse models of retinal degeneration (Neves et al., 2016). Since MANF supplementation was sufficient to prevent retinal damage in response to light exposure in old mice (Fig. 2) we asked whether MANF treatment could also improve repair capacity in the old retina following transplantation of photoreceptors. By comparing two cohorts of old mice that received the same Nrl-GFP+ cell suspension with and without hrMANF supplementation (one single subretinal injection), we found a significant increase in the number of GFP+ cells in the ONL of mice that received MANF–supplemented transplants (Fig. 3c-d, see also Supplemental Fig. S3a), suggesting an improved repair capacity of the old retina treated

with hrMANF. To qualitatively evaluate the overall ability of MANF to improve the repair capacity in the old retina, we categorized all animals analyzed in this study (See Supplemental Fig. S3a for full data set) into repair efficiency categories (low, <500 GFP+ cells to very high>1500 GFP+ cells). This analysis demonstrated that more than 50% of old eyes showed low repair capacity, but MANF supplementation was sufficient to significantly shift this outcome to high or very high levels of repair capacity, approaching the profile that is observed in young animals (Fig. 3e).

In young animals, the effects of MANF on retinal transplants depend on immune modulation: integration efficiency is impaired in mice carrying MANF-irresponsive macrophages (Cx3Cr1- null mice, see (Neves et al., 2016) and, in this immune-deficient setting, MANF supplementation does not improve integration efficiency (Supplemental Figure S3b-c). Consistent with a mechanism involving immune modulation, we also observed a reduction of CD68+ cells in the sub retinal space surrounding GFP+ cells in MANF supplemented eyes (Fig. 3f): while CD68+ cells only appear occasionally in transplant sites in young mice, and untreated old mice exhibit increased densities of CD68+ macrophages in the sub-retinal space, old eyes that received MANF-supplemented transplants had a reduced or absent number of CD68+ macrophages. This suggests that, in old mice, the ability to achieve retinal repair may also depend on immune modulation.

Discussion

Collectively, our data show that ageing alone, in the absence of any disease-associated genetic alterations, is sufficient to impair retinal homeostasis, increasing the susceptibility to retinal degeneration and to limit the retinal repair capacity necessary for regenerative strategies. Age-associated loss of MANF may be one of the underlying causes of this dysfunction as mice with reduced MANF levels have enhanced susceptibility to retinal degeneration (Neves et al., 2016) and accelerate the development of immune dysfunctions observed in old mice (Fig. 1). Moreover, MANF supplementation is sufficient to reduce retinal damage induced by light exposure in old retinae (Fig. 2) and increase retinal repair after photoreceptor transplant in old mice (Fig. 3).

While whole organ levels of MANF protein decline with age in many other tissues (Sousa-Victor et al., 2019), this was not the case within the eye, and the age-associated reduction in MANF levels was restricted to the choroid (Fig.1), perhaps reflecting the age-related decline in the circulatory levels of MANF (Sousa-Victor et al., 2019). The mechanistic basis for the age-related decline in MANF levels is still unknown and may explain why different tissue compositions might affect the overall decline in whole organ content of MANF protein. Considering that immune cells reside within the choroid blood vessels and that MANF immune modulatory signaling is needed to limit inflammatory activation, the decline in MANF levels may contribute to the pathological accumulation of pro-inflammatory macrophages in the retina, as supported by our analysis of MANF loss of function models. Moreover, since the beneficial effects of MANF in retinal repair depend on immune modulation (Neves et al., 2016), it is possible that lack of this immune modulatory effect in the immune cells from old mice could underlie, at least in part, the defects in retinal homeostasis and repair that we observe.

The loss of MANF during ageing is accompanied by alterations in immune signaling in the retina (Chen et al., 2010), including changes in Cx3cl1 (reduction) and Ccl2 (increase) expression (Fig. 1a). Loss of function of Cx3cr1 is one of the genetic hallmarks in AMD (Combadiere et al., 2007) and mouse models used to mimic some aspects of the disease demonstrate a similar dichotomy in these signaling systems, showing Ccr2+ inflammatory monocytes infiltrates in Cx3Cr1-deficient mice, which develop some aspects of the disease (Sennlaub et al., 2013). At 12 months of age, there is not yet increased susceptibility of the retina to degeneration in response to light exposure, which is only observed at this age in Cx3Cr1-deficient mice (Sennlaub et al., 2013). Thus, it is possible that the immune environment that develops during physiological ageing synergizes with specific genetic alterations that occur in AMD patients to amplify the immune defects that lead to photoreceptor loss.

In the context of cell replacement therapies, our data support the notion that immune modulation may also be an effective way to improve the success of repair when retinal transplants are applied to aged patients, and thus a possible strategy to increase the chance of restoring vision in patients where vision impairments are primarily driven by photoreceptor loss. In mice, age-related vision loss is not always observed and it depends on multiple factors, including a central nervous system component that is independent of retinal health (Lehmann et al., 2012). Thus, evaluation of vision function in old mice that received transplants will not be informative on the success of this particular therapeutic approach. Nevertheless, in mouse models where vision impairments are driven by photoreceptor loss it has been consistently demonstrated that photoreceptor supplementation is sufficient to restore vision (Barber et al., 2013; MacLaren et al., 2006; Neves et al., 2016; Santos-Ferreira et al., 2015; Zhu et al., 2017). Although there is extensive debate regarding the cellular mechanism involved in retinal repair following transplantation (Santos-Ferreira et al., 2016), it has been consistently demonstrated by different groups that the extent of vision recovery following transplantation positively correlates with the number of GFP+ cells in the ONL after transplant (Barber et al., 2013; MacLaren et al., 2006; Neves et al., 2016; Santos-Ferreira et al., 2015; Zhu et al., 2017). Thus, evaluating the number of GFP+ cells residing in the ONL of treated mice can be taken as an indicator of the success of retinal repair. As we observe a significant increase in the number of GFP cells in the ONL of old mice following MANF-supplemented transplants, we propose that the use of this co-adjuvant in retinal transplants may have a beneficial effect in the clinic when treating old patients where vision loss is primarily driven by photoreceptor loss. Importantly, our data suggest that in Cx3cr1 loss of function conditions, where macrophages are MANF irresponsive (Neves et al., 2016), MANF supplementation does not improve integration efficiency of photoreceptors. Thus, in clinical conditions of AMD where misexpression and polymorphisms in Cx3cr1 is one of the genetic factors (Falk et al., 2014; Tuo et al., 2004), concurrent interventions will likely be required to reestablish the capacity of macrophages to respond to MANF signals. Designing such strategies will require a better understanding of the molecular mechanisms of action of MANF protein.

One other factor to take into consideration when applying this strategy to old organisms, is the fact that MANF decline with ageing occurs at the systemic level. Thus, while local MANF supplementation may contribute to increased repair capacity following transplants,

the long term maintenance of these effects may be compromised by the inflammatory systemic environment present in the old animal. Regulation of inflammatory signaling is emerging as a path for rejuvenation (Neves and Sousa-Victor, 2020) and we already demonstrated that systemic delivery of MANF protein is an effective strategy to allay age-related inflammation and reestablish immune homeostasis (Sousa-Victor et al., 2019). It would be interesting to combine systemic MANF interventions with MANF supplemented transplants as a means to increase the success of long term repair of the retina in old organisms.

While the molecular mechanism underlying MANF function is still unclear, the application of this factor to promote repair and reduce inflammation in ageing is now starting to emerge (Sousa-Victor et al., 2018; Sousa-Victor et al., 2019). As a systemic regulator of immune homeostasis, MANF has the potential to affect multiple systems in the body and may, thus, be envisioned as a general promoter of tissue repair in old organisms (Neves and Sousa-Victor, 2020). Here we show that, at least in the retina, it can be used to limit age-related susceptibility to tissue damage and can also function as an important co-adjuvant to overcome the roadblocks imposed by ageing to regenerative therapies (Fig. 4).

Materials and Methods

Experimental animals

All mice used in the described studies were housed at the AAALAC accredited vivarium of The Buck Institute for Research on Aging in a Specific Pathogen Free (SPF) facility, in individually ventilated cages on a standard 12:12 light cycle. All procedures were approved by the Buck Institute Institutional Animal Care and Use Committee (IACUC).

Young and old mice used in this study were C57BL/6NJ mice without the Rd8 mutation, obtained from the National Institute of Ageing or bred in house.

Manf heterozygous mice used for analysis at middle age and Cx3cr1-deficient mice used for subretinal transplants have been previously described (Neves et al., 2016). Manf heterozygous mice obtained from UC Davis KOMP Repository Knockout mouse project (clone MANF_D06 (EPD0162_3_D06; C57Bl/6N-Manftm1a(KOMP)Wtsi) were generated in a C57Bl/6N background and backcrossed into C57Bl/6J in our facilities to eliminate the Rd8 mutation in the crb1 allele. All mice used in the experiments were littermates from Manf +/− crosses and all were negative for the Rd8 mutation, which affects retinal phenotypes (Mattapallil et al., 2012). Primers used for genotyping for the Manf allele (wt vs. null) and the crb1 allele (rd8 mutation vs. wt) are listed in Table S1.

Cx3Cr1−/− mice are B6.129P2(Cg)-Cx3Cr1tm2.1(CRE/ERT)Litt/WganJ and were purchased from The Jackson Laboratory (JAX, stock nr. 021160). In these mice, a CreER-IRES-EYFP cassette replaces the first 390 bp of the second Cx3Cr1 exon, encoding the N terminus of the seven-transmembrane receptor shown to be crucial for interaction with FKN. These mice have been previously characterized and the null allele validated (Jung et al., 2000; Parkhurst et al., 2013). Primers used for genotyping for the Cx3Cr1 allele (wt vs. null) are listed in Table S1.

Intraocular Injections in mice

hrMANF protein for intraocular injections—hrMANF (Icosagen AS, Tartu, Estonia, Batch 030513): Human recombinant mesencephalic astrocyte-derived neurotrophic factor was a kind gift from Amarantus Biosciences Inc. hrMANF was expressed by in a Chinese hamster ovary (CHO)-based cell line using QMCF technology and purified by ion-exchange and gel-filtration chromatography from serum-free CHO growth medium. hrMANF was provided as a 1mg/ml solution in PBS, pH 7.4. Vehicle for all experiments was sterile PBS (Phosphate Buffered Saline, Corning).

Preparation of Nrl-GFP cells for subretinal injection—Retinas of P4-P6 Nrl-GFP mice were dissected in a chilled 1x Hank's Balanced Salt Solution (HBSS). Each retina was incubated in 700ul of Papain solution (Worrington, Cat# 3176, reconstituted in 5ml of 1X EBSS) for 30 minutes at 37°C, and mechanically dissociated every 10min by pipetting. Papain was inactivated by adding an equal volume of Papain inhibitor Ovomucoid-albumin (Worrington, Cat# 3182, reconstituted at 10mg/ml in EBSS), 100ul of Fetal Bovine Serum (FBS, J R Scientific, Woodland, CA) and 5ul of DNAse solution (1 unit/ul). Cells were recovered by centrifugation at 1200 rpm for 3 min. The cell pellet was re-suspended in 12ul of DMEM/F-12 containing 1% Sodium Pyruvate, 1% of HEPES, 1% of Essential amino acid, 2% glucose, 1% Sodium Bicarbonate, 1% Penicillin/Streptomycin, 0.5% FBS and 1% N2 supplement, and each 10ul aliquot of cell suspension was further supplemented with either 4ul of hrMANF (1ug/ul) or PBS immediately before subretinal injection.

Intravitreal injection procedure—Animals were anesthetized using isoflurane and kept under anesthesia during the procedure. Following testing the depth of anesthesia, 1μl of hrMANF or vehicle were delivered in one single injection into the right eye using a graduated pulled glass pipet and a wire plunger (Wiretrol II, 5-0000-2005, Drummond Scientific Company). The pipet was used to poke a hole just beyond the corneo-scleral margin, further advanced carefully, and the solution delivered into the vitreous space. The pipet was kept in place for 30secs for the intra-ocular pressure to normalize and then gently withdrawn.

Subretinal Injection procedure—Dissociated GFP-expressing mouse retinal cells from the Nrl-GFP mice were transplanted into the subretinal space of recipient mice of different ages. Animals were anesthetized using isoflurane and kept under anesthesia during the procedure. Following testing the depth of anesthesia, the subretinal space was reached by an incision in the sclera, choroid and RPE of the dorsal eye, near the ora serrata. 2μl of cell suspension (7.5×10^5 cells) was slowly injected using a pulled fine glass micropipette with a wire plunger (Wiretrol II, 5-0000-2005, Drummond Scientific Company). Each animal received one single injection of cell suspension with or without MANF supplementation. Animals were analyzed 14 days after subretinal injections.

After both types of injections, eyes were coated with antibiotic ointment (Neomycin and polymyxin B Sulfates and Bacitracin Zinc ophthalmic Ointment, USP, 1748-235-35, Akorn) and animals were allowed to recover on a warm pad before being transferred to their cages.

Light exposure in mice

Mice were dark adapted for 18h before the procedure. Animals were anesthetized for 15 min in an isoflurane chamber and pupils were dilated using a mixture of 5% Phenylephrine (Arcos Organics) and 1% Tropicamide (Alfa Aesar). When intravitreal injections were performed in combination, animals were injected prior to light exposure. Test eyes were exposed to 15,000 lux of bright light for 2h. Mice were kept under anesthesia during light exposure to ensure direct and constant illumination during the exposure time. Light intensity at the site of exposure was measured using a digital lux meter (LX1330B, Sinometer). After light exposure, mice were allowed to recover from anesthesia, returned to their cages and housed in darkness until analysis. Unexposed control mice were housed in regular conditions (see above) throughout the experiment. All animals were analyzed 48h after light exposure.

Reverse-Transcription and Real-Time quantitative PCR (RT-qPCR)

Total RNA was extracted from flash frozen whole eyes using TRIzol and cDNA was synthesized using 1000ng of RNA and iScript cDNA synthesis kit (BioRad). Real-time PCR was performed on a Bio-Rad CFX96TM detection system, using SsoAdvanced™ Universal SYBR® Green Supermix (BioRad). Quantification of expression for each gene in each sample was normalized to beta-actin and results are shown as gene expression levels in samples from old animals relative to levels in samples from young animals which are arbitrarily set to one. Each gene was quantified in samples obtained from 4 different eyes from animals at each age. For information on primer sequences see Table S2.

MANF protein quantification in whole eye protein extracts by ELISA

Whole eyes were homogenized in IP buffer supplemented with protease inhibitors (Sigma) and phosphatase inhibitors (Sigma) for 45 min at 4°C and supernatant protein extracts were recovered by centrifugation. Protein concentration in samples was determined using Protein coomassie assay reagent (ThemoScientific). MANF concentrations in protein samples were determined with MyBiosource mouse MANF ELISA kit (MyBiosource, MBS2025592) in samples diluted 1:1 in PBS supplemented with protease inhibitors (Sigma), according to manufacturer's instructions. MANF concentration was normalized to total protein concentration in each sample. For each age MANF was quantified in 10 samples originating from independent eyes.

Histological analysis, Imaging and quantification methods in mouse tissues

Mouse eye tissue harvesting and storage—Whole eyes were dissected out from treated animals at the designated times and fixed overnight at 4°C in 4% Paraformaldehyde in PBS (4%PFA) with a small incision in the cornea to allow intraocular access to fixative. After fixation, the cornea and lens were dissected out and the retinal tissue fixed for an additional hour in fresh 4% PFA. The tissue was washed 3 times with PBS and incubated with 15% sucrose in PBS overnight at 4°C. Sucrose treated tissue was embedded in 7.5% gelatin/15% sucrose in PBS at 37°C for 2h and then transferred to cryomolds (Tissuetek) and flash frozen with 2-methylbutane at −80°C. Frozen embedded tissue was cryosectioned

at 14um thickness, collected in Superfrost Plus microslides (VWR) and stored at −80°C until analysis.

IHC of mouse eye cryosections and nuclei staining—Cryosections collected in slides were thawed and hydrated in PBS for 15 minutes at room temperature (RT). For antibody staining, sections were permeabilized with PBS containing 0.1% Tween20 (PBT) for 15 min at RT, blocked with 10% donkey serum (Jackson ImmunoResearch) in PBT and incubated with primary antibody, diluted in blocking solution, overnight at 4°C. Primary antibody was washed 3 times with PBT and detected using Alexa conjugated secondary antibodies (Invitrogen, Molecular Probes). Secondary antibody was washed 6 times with PBT. For nuclei staining, slides were incubated for 5min in 300nM DAPI (4',6-diamidino-2-phenylindole) in PBS at RT, rinsed in PBS and mounted with Fluoromount G media (17984-25, Electron Microscopy Sciences) and micro cover glass No. 2 (48382-128, VWR). Primary antibodies used were as follows: rabbit anti-MANF (1:300; Sigma, SAB3500384); rat anti-CD68 (1:100, AbD Serotec (FA-11)); goat anti-IBA1 (1:100; Novus Biologicals, NB1001028SS); and goat anti-GFP (1:800; NB 100-1770, Novus Biologicals).

TUNEL staining of mouse eye cryosections—Cryosections collected in slides were thawed and hydrated in PBS for 15 minutes at room temperature (RT). Tissue was permeabilized for 2 min in boiling 10mM Citrate buffer and washed 3 times with PBS after cooling down to RT. Cryosections were incubated in the dark for 1h at 37 degrees Celsius with 50ul of TUNEL reaction mixture (In situ cell death detection kit, TMR Red, Roche) prepared according to manufacturer's instructions. Slides were rinsed three times with PBS, counterstained with DAPI and mounted as described above.

Imaging—All preparations were imaged using a Zeiss LSM 700 confocal laser scanning microscope.

Quantification of MANF and CD68 staining intensity in whole eye sections—For MANF, quantifications were performed in 1024x1024px fields from confocal captures of the fluorescent signal originating from MANF immune staining, using image J. Rectangular shapes were used to define the different eye regions and the whole area of ocular tissue and mean intensity of the fluorescent signal was quantified, after threshold normalization, for 5 independent eyes at each age.

For CD68, quantifications were performed in whole eye sections reconstructed from overlay of 1024x1024px fields from confocal captures, using image J. Total eye area area was drawn based on DAPI staining and CD68 signal intensity within the area defined was quantified after threshold normalization, for 4 independent eyes at each age.

Quantification of TUNEL nuclei—TUNEL+ nuclei were counted directly under the microscope in whole eye sections stained with TUNEL and DAPI. Quantifications include 25 independent sections per eye, covering 2/3 of the retina, in a total of 5-7 eyes/condition, collected in two independent experiments.

Quantification of immune cells in the eye—The total numbers of CD68+, MANF+ and Iba-1+ cells in the choroid were counted in micrographs captured from cryosections double-stained with the corresponding antibodies. Choroid region was identified and the area of the choroid region, in each micrograph, was determined using ImageJ, after scale normalization. The total number of Iba-1+, CD68+, and double-labeled cells were counted for each micrograph, normalized to the area, and averaged for each animal. Quantifications are of 2-4 images/eye and 3-4 eyes/age or genotype.

The total numbers of CD68+ cells in the ONL (Fig. 2c) were counted directly under the microscope in whole eye sections stained with an anti-CD68 antibody. Co-staining with DAPI was used to identify nuclei. Quantifications include at least 5 independent sections per eye, in a total of 7-8 eyes/condition, collected in at least two independent experiments.

Quantification of cell integration in subretinal injections—Successful subretinal injections were determined by detecting the presence of GFP expressing cells in the subretinal space. For eyes with successful injections, retinas were serially sectioned in about 50 slides with 4 sections/slide and every 4th slide was stained with an antibody against GFP and DAPI. The number of integrated cells was quantified in all sections observed under the microscope. Cells were considered integrated if they were present within two rows of the host ONL as defined by DAPI staining. The total number of integrated cells/eye was extrapolated from the total number of slides/eye. Quantifications include 4-10 eyes/condition from 2-4 independent experiments. See supplemental Figure S3a for detailed description of groups analyzed in each experiment.

Human retinal tissue analysis

Human tissue collection—Human eyes were obtained through our collaboration with Dr. Robert Mullins lab from the University of Iowa (Iowa City, IA, USA), after receiving informed consent from the donors' families, and all experiments comply with the Declaration of Helsinki. Eyes from donors with normal ocular history were utilized for immunohistochemical studies. To obtain ocular tissue, which spans from the neural retina and includes the RPE, choroid and sclera, 8mm-diameter punches, centered around the fovea centralis, were collected for analysis of the macula. An extramacular wedge of retinal tissue was also obtained for two of the control donors.

Immunohistochemistry in human tissue—Human retina/RPE-choroid tissue was fixed in 4% paraformaldehyde before running the tissue through a sucrose gradient for cryopreservation. The tissue was embedded in 20% sucrose in O.T.C. compound (VWR, Radnor, PA), and subsequently cryosectioned to generate 7μm-thick sections. Sections were blocked using 0.1% BSA (Sigma, A3294) in 1x PBS with 1mM $MgCl_2$ and 1mM $CaCl_2$ for 15 minutes, followed by primary antibody incubation with rabbit anti-MANF (1:100; Sigma, SAB3500384), goat anti-IBA1 (1:100; Novus Biologicals, NB1001028SS), and the lectin *Ulex europaeus* agglutinin I (UEA-I, 1:50; Vector Laboratories, B-1065) for 2 hours at room temperature. Alexa Fluor secondary antibodies, 488 donkey anti-rabbit (1:200; Life Technologies, A21206), 555 donkey anti-goat (1:200; Life Technologies, A21432), and 647 streptavidin (1:200; Jackson ImmunoResearch, 016-600-084) were applied to the sections

for 30 minutes at room temperature. DAPI (0.5μg/mL; Roche, 10236276001) was then used to counterstain nuclei with a 5-minute incubation. Coverslips were mounted on the slides using Fluoromount-G (Electron Microscopy Sciences, 17984-25). All antibodies, as well as DAPI, were diluted in 1x PBS containing 1mM $MgCl_2$ and 1mM $CaCl_2$. Images were collected using a ZEISS LSM 700 confocal microscope.

Statistical Analysis

All data are presented as average and standard error of mean (s.e.m.). Statistical analysis was carried out using Microsoft Excel or GraphPad Prism 5. For comparisons between two groups, two-tailed Student's t-test was used to determine statistical significance, assuming normal distribution and equal variance. For multiple comparisons, one-way ANOVA with Dunnett's multiple comparison post-test was used to determine statistical significance. Statistical analysis of cell integration after subretinal transplants was done between groups that were generated within the same experiment, which received the same cell suspension. Thus, for each comparison between 2 groups, quantifications for a certain experimental group obtained in experiments where the other experimental group was not present were excluded from the statistical analysis.

Supplementary Material

Refer to Web version on PubMed Central for supplementary material.

Acknowledgments

We acknowledge Dr. Robert Mullins from the University of Iowa for kindly providing the human samples analyzed in this study. We acknowledge Amarantus Biosciences Inc. for kindly supplying the hrMANF protein used in these studies. This work was supported by NIH grants EY025779 to D.A.L. and NIH grants AG052989 and AG047497 to H.J. J.N. was supported by the Glenn Foundation for Medical Research. This work was made possible, in part, by NEI P30 EY002162 - Core Grant for Vision Research, and by an unrestricted grant from Research to Prevent Blindness, New York, NY

References

Ambati J, Atkinson JP, and Gelfand BD (2013). Immunology of age-related macular degeneration. Nature reviews Immunology 13, 438–451.

AMD Alliance International (2010). The Global Economic Cost of Visual Impairment [online]. http://wwwicophorg/resources/146/The-Global-Economic-Cost-of-Visual-Impairmenthtml.

Ardeljan D, and Chan CC (2013). Aging is not a disease: distinguishing age-related macular degeneration from aging. Progress in retinal and eye research 37, 68–89. [PubMed: 23933169]

Barber AC, Hippert C, Duran Y, West EL, Bainbridge JW, Warre-Cornish K, Luhmann UF, Lakowski J, Sowden JC, Ali RR, et al. (2013). Repair of the degenerate retina by photoreceptor transplantation. Proceedings of the National Academy of Sciences of the United States of America 110, 354–359. [PubMed: 23248312]

Cao X, Shen D, Patel MM, Tuo J, Johnson TM, Olsen TW, and Chan CC (2011). Macrophage polarization in the maculae of age-related macular degeneration: a pilot study. Pathology international 61, 528–535. [PubMed: 21884302]

Chen M, Muckersie E, Forrester JV, and Xu H (2010). Immune activation in retinal aging: a gene expression study. Investigative ophthalmology & visual science 51, 5888–5896. [PubMed: 20538981]

Combadiere C, Feumi C, Raoul W, Keller N, Rodero M, Pezard A, Lavalette S, Houssier M, Jonet L, Picard E, et al. (2007). CX3CR1-dependent subretinal microglia cell accumulation is associated

with cardinal features of age-related macular degeneration. The Journal of clinical investigation 117, 2920–2928. [PubMed: 17909628]

Cruz-Guilloty F, Saeed AM, Echegaray JJ, Duffort S, Ballmick A, Tan Y, Betancourt M, Viteri E, Ramkhellawan GC, Ewald E, et al. (2013). Infiltration of proinflammatory m1 macrophages into the outer retina precedes damage in a mouse model of age-related macular degeneration. International journal of inflammation 2013, 503725. [PubMed: 23533946]

Falk MK, Singh A, Faber C, Nissen MH, Hviid T, and Sorensen TL (2014). CX3CL1/CX3CR1 and CCL2/CCR2 chemokine/chemokine receptor complex in patients with AMD. PloS one 9, e112473. [PubMed: 25503251]

Gao FJ, Wu JH, Li TT, Du SS, and Wu Q (2017). Identification of Mesencephalic Astrocyte-Derived Neurotrophic Factor as a Novel Neuroprotective Factor for Retinal Ganglion Cells. Frontiers in molecular neuroscience 10, 76. [PubMed: 28367115]

Gao FJ, Zhang SH, Li TT, Wu JH, and Wu Q (2016). Expression and Distribution of Mesencephalic Astrocyte-Derived Neurotrophic Factor in the Retina and Optic Nerve. Frontiers in human neuroscience 10, 686. [PubMed: 28154531]

Geissmann F, Jung S, and Littman DR (2003). Blood monocytes consist of two principal subsets with distinct migratory properties. Immunity 19, 71–82. [PubMed: 12871640]

Jung S, Aliberti J, Graemmel P, Sunshine MJ, Kreutzberg GW, Sher A, and Littman DR (2000). Analysis of fractalkine receptor CX(3)CR1 function by targeted deletion and green fluorescent protein reporter gene insertion. Molecular and cellular biology 20, 4106–4114. [PubMed: 10805752]

Lamba DA, Gust J, and Reh TA (2009). Transplantation of human embryonic stem cell-derived photoreceptors restores some visual function in Crx-deficient mice. Cell stem cell 4, 73–79. [PubMed: 19128794]

Lehmann K, Schmidt KF, and Lowel S (2012). Vision and visual plasticity in ageing mice. Restorative neurology and neuroscience 30, 161–178. [PubMed: 22348872]

Lu J, Luo L, Huang D, Liu X, Xia X, Wang Z, Lam BL, Yi J, Wen R, and Li Y (2018). Photoreceptor Protection by Mesencephalic Astrocyte-Derived Neurotrophic Factor (MANF). eNeuro 5.

MacLaren RE, Pearson RA, MacNeil A, Douglas RH, Salt TE, Akimoto M, Swaroop A, Sowden JC, and Ali RR (2006). Retinal repair by transplantation of photoreceptor precursors. Nature 444, 203–207. [PubMed: 17093405]

Mandai M, Watanabe A, Kurimoto Y, Hirami Y, Morinaga C, Daimon T, Fujihara M, Akimaru H, Sakai N, Shibata Y, et al. (2017). Autologous Induced Stem-Cell-Derived Retinal Cells for Macular Degeneration. The New England journal of medicine 376, 1038–1046. [PubMed: 28296613]

Mattapallil MJ, Wawrousek EF, Chan CC, Zhao H, Roychoudhury J, Ferguson TA, and Caspi RR (2012). The Rd8 mutation of the Crb1 gene is present in vendor lines of C57BL/6N mice and embryonic stem cells, and confounds ocular induced mutant phenotypes. Investigative ophthalmology & visual science 53, 2921–2927. [PubMed: 22447858]

Neves J, and Sousa-Victor P (2020). Regulation of inflammation as an anti-aging intervention. The FEBS journal 287, 43–52. [PubMed: 31529582]

Neves J, Sousa-Victor P, and Jasper H (2017). Rejuvenating Strategies for Stem Cell-Based Therapies in Aging. Cell stem cell 20, 161–175. [PubMed: 28157498]

Neves J, Zhu J, Sousa-Victor P, Konjikusic M, Riley R, Chew S, Qi Y, Jasper H, and Lamba DA (2016). Immune modulation by MANF promotes tissue repair and regenerative success in the retina. Science 353, aaf3646. [PubMed: 27365452]

Parkhurst CN, Yang G, Ninan I, Savas JN, Yates JR 3rd, Lafaille JJ, Hempstead BL, Littman DR, and Gan WB (2013). Microglia promote learning-dependent synapse formation through brain-derived neurotrophic factor. Cell 155, 1596–1609. [PubMed: 24360280]

Peng B, Xiao J, Wang K, So KF, Tipoe GL, and Lin B (2014). Suppression of microglial activation is neuroprotective in a mouse model of human retinitis pigmentosa. The Journal of neuroscience : the official journal of the Society for Neuroscience 34, 8139–8150. [PubMed: 24920619]

Perez VL, and Caspi RR (2015). Immune mechanisms in inflammatory and degenerative eye disease. Trends in immunology 36, 354–363. [PubMed: 25981967]

Santos-Ferreira T, Postel K, Stutzki H, Kurth T, Zeck G, and Ader M (2015). Daylight vision repair by cell transplantation. Stem Cells 33, 79–90. [PubMed: 25183393]

Santos-Ferreira TF, Borsch O, and Ader M (2016). Rebuilding the Missing Part-A Review on Photoreceptor Transplantation. Frontiers in systems neuroscience 10, 105. [PubMed: 28105007]

Sennlaub F, Auvynet C, Calippe B, Lavalette S, Poupel L, Hu SJ, Dominguez E, Camelo S, Levy O, Guyon E, et al. (2013). CCR2(+) monocytes infiltrate atrophic lesions in age-related macular disease and mediate photoreceptor degeneration in experimental subretinal inflammation in Cx3cr1 deficient mice. EMBO molecular medicine 5, 1775–1793. [PubMed: 24142887]

Sousa-Victor P, Jasper H, and Neves J (2018). Trophic Factors in Inflammation and Regeneration: The Role of MANF and CDNF. Frontiers in physiology 9, 1629. [PubMed: 30515104]

Sousa-Victor P, Neves J, Cedron-Craft W, Ventura PB, Liao C, Riley RR, Soife I, van Bruggen N, Kolumam GA, Villeda SA, et al. (2019). MANF regulates metabolic and immune homeostasis in ageing and protects against liver damage. Nat Metab 1, 276–290. [PubMed: 31489403]

Tuo J, Smith BC, Bojanowski CM, Meleth AD, Gery I, Csaky KG, Chew EY, and Chan CC (2004). The involvement of sequence variation and expression of CX3CR1 in the pathogenesis of age-related macular degeneration. FASEB journal : official publication of the Federation of American Societies for Experimental Biology 18, 1297–1299. [PubMed: 15208270]

Wenzel A, Reme CE, Williams TP, Hafezi F, and Grimm C (2001). The Rpe65 Leu450Met variation increases retinal resistance against light-induced degeneration by slowing rhodopsin regeneration. The Journal of neuroscience : the official journal of the Society for Neuroscience 21, 53–58. [PubMed: 11150319]

West EL, Pearson RA, Barker SE, Luhmann UF, Maclaren RE, Barber AC, Duran Y, Smith AJ, Sowden JC, and Ali RR (2010). Long-term survival of photoreceptors transplanted into the adult murine neural retina requires immune modulation. Stem Cells 28, 1997–2007. [PubMed: 20857496]

Zhu J, Cifuentes H, Reynolds J, and Lamba DA (2017). Immunosuppression via Loss of IL2rgamma Enhances Long-Term Functional Integration of hESC-Derived Photoreceptors in the Mouse Retina. Cell stem cell 20, 374–384 e375. [PubMed: 28089909]

Highlights

- Ageing is associated with a reduction in MANF protein levels and increased densities of activated macrophages in the choroid of mice and humans.
- Ageing limits retinal homeostatic capacity following light exposure and reduces the efficiency of cell replacement therapies applied to the mouse retina.
- MANF supplementation reduces the numbers of activated macrophages within the eye of old animals and improves retinal homeostasis and repair capacity.
- MANF therapy is a potential intervention to maintain retinal homeostasis in the elderly and improve the success of retinal regenerative therapies applied to aged individuals.

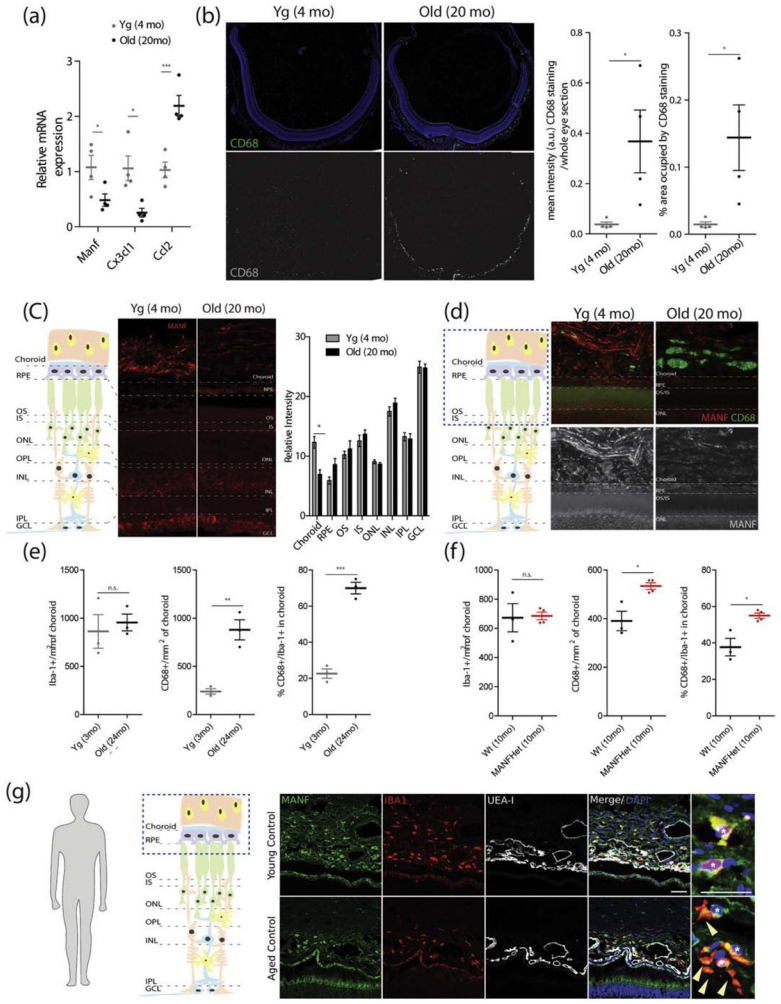

Figure 1: MANF protein levels decline with age in the retinal choroid of mice and humans.

(a) Relative levels of Manf, Cx3cl1 and Ccl2 transcripts, quantified by RT-qPCR, in whole eyes from young (4mo) and old (20mo) mice (n=4/age). (b) Representative images of whole eye cryosections of young (4mo) and old (20mo) mice immunostained against CD68 (green). DAPI shows nuclear staining. Quantifications of these stainings, for independent animals, as the mean intensity of the fluorescent signal within the whole eye section and the percent of eye area occupied by the fluorescent signal (n=4/age) are shown. See also Supplemental Figure S1. (c) Representative images of cryosections from whole eyes of young (4mo) and old (20mo) mice immunostained against MANF (red). Diagram to the left is a cartoon representing the different retinal layers analyzed and the choroid. Quantifications of these stainings, for independent animals, as the mean intensity of the fluorescent signal, within the different regions is shown on the right (n=5/age). See also Supplemental Figure S2b. (d) Representative images of cryosections from whole eyes of young (4mo) and old (20mo) mice immunostained against MANF (red) and CD68 (green). Image shows a high magnification detail of the choroid region, as indicated in the diagram on the left. (e,f) Quantification of the total number of Iba-1+ (left) and CD68+ (middle) immune cells and the percentage of Iba-1+ cells positive for CD68 (right) in the choroid of

young (3mo) and old (24mo) mice (e) or of middle aged (10mo) MANFHet mice and wt littermates (f). See also Supplemental Figures S2d-e. (g) Representative images of cryosections from ocular tissue of young and aged non-diseased human donors immunostained against MANF (green), IBA1 (red) and UEA-1 (white). Image shows a detail of the choroid region as indicated in the diagram on the left. Nuclear staining with DAPI is shown in blue. See also Supplemental Figure S2f. Data are represented as average ± s.e.m. and each n represents one animal. p values are from two-tailed Student's t-test.

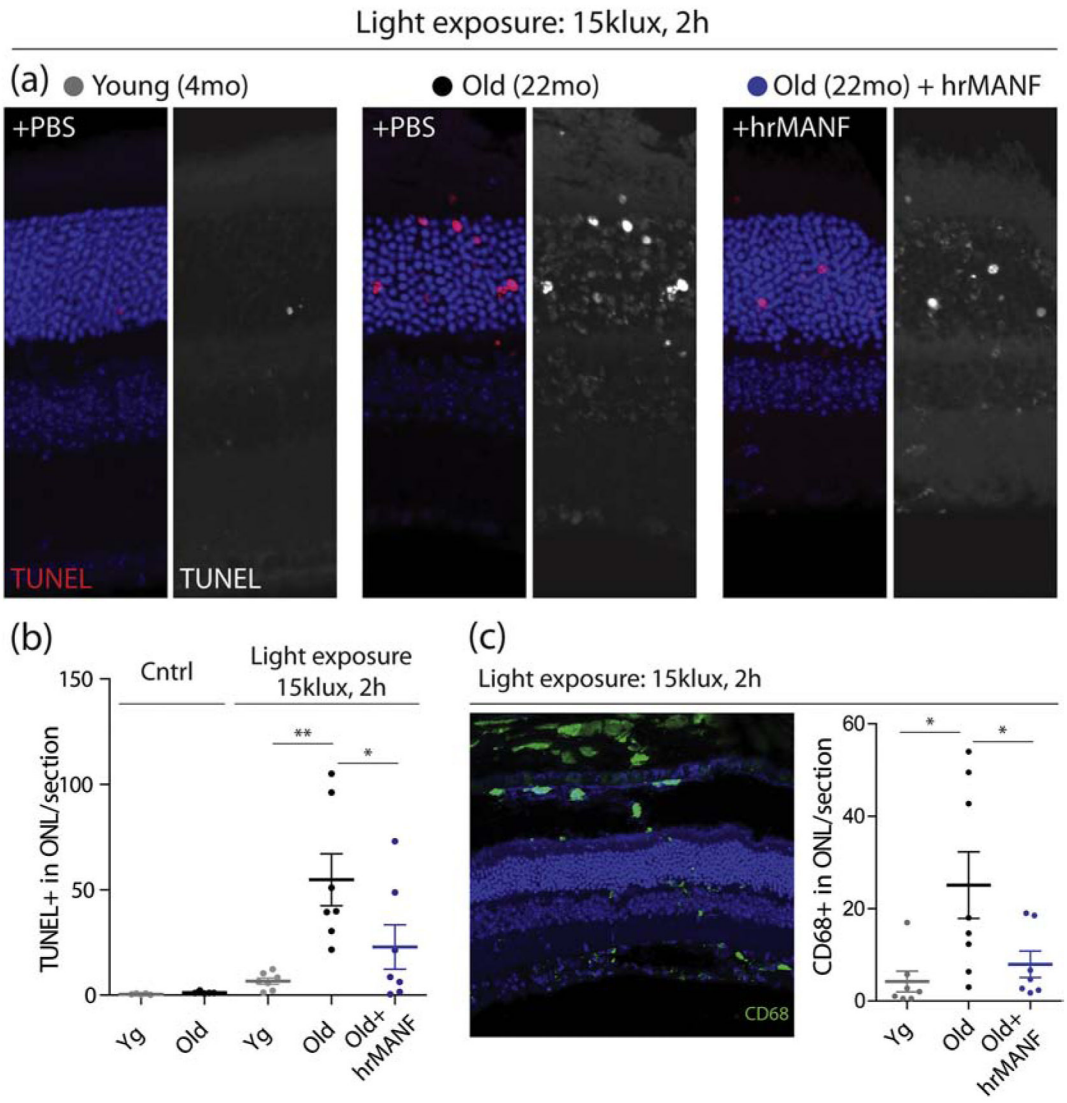

Figure 2: Ageing increases susceptibility to light damage in the retina and can be reduced by MANF supplementation.

(a) Representative images of cryosections, with TUNEL staining (red/white), from retinae of young (4mo) and old (22mo) mice, 48h after exposure to 15klux for 2h. Some old mice received one intravitreal injection of hrMANF prior to light exposure (old +hrMANF). Nuclear staining with DAPI is shown in blue. (b) Quantification of the average number of TUNEL+ nuclei in the ONL per section, in retinae of young (4mo) and old (22mo) mice, 48h after exposure to 15klux for 2h. Some old mice received one intravitreal injection of hrMANF prior to light exposure (old + hrMANF) (no light exposure: n=5/age; light exposure: n=7/condition). (c) Quantification of the average number of CD68+ cells in the ONL, per section, in retinae of young (4mo) and old (22mo) mice, 48h after exposure to 15klux for 2h. Some old mice received one intravitreal injection of hrMANF prior to light exposure (old + hrMANF) (n=7-8/condition). On the left it is shown a representative image of CD68+ cells present in the ONL of an old (22mo) mouse, 48h after exposure to 15klux

for 2h. Data are represented as average ± s.e.m. and each n represents one animal. p values are from one-way ANOVA with Dunnett's multiple comparison post-test.

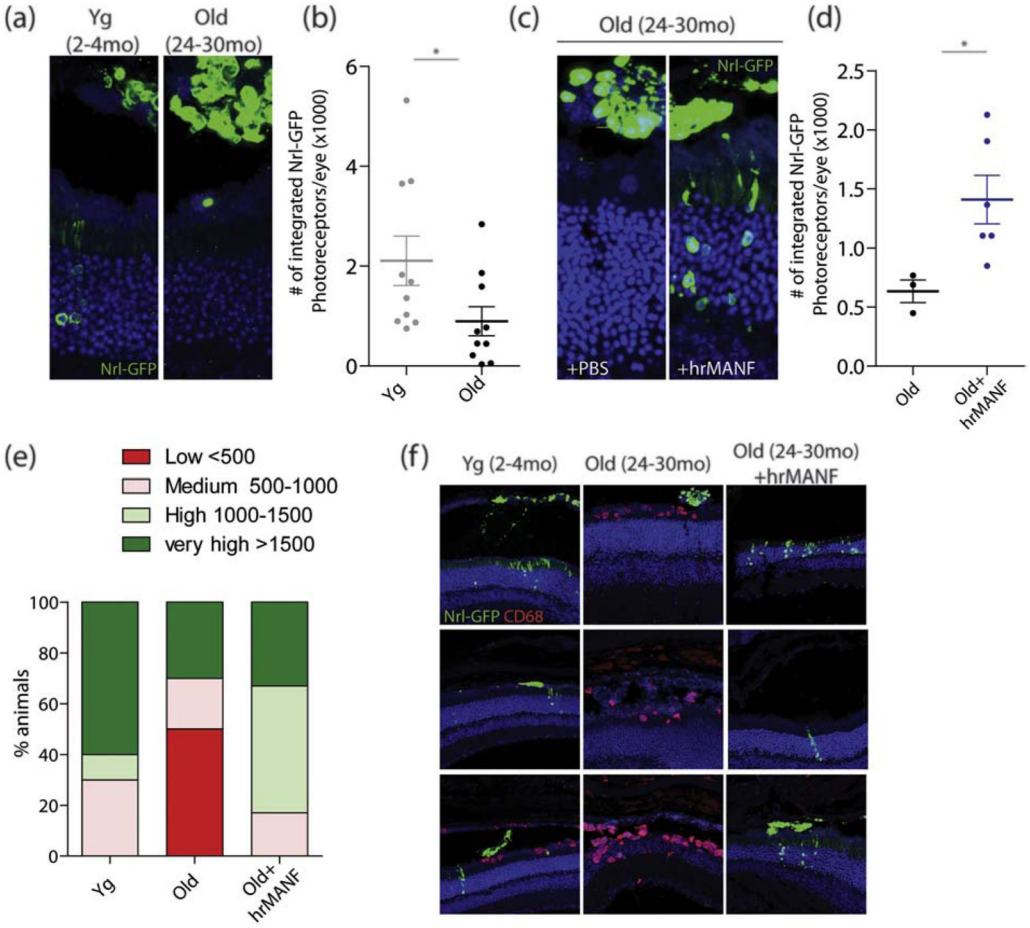

Figure 3: Ageing reduces the efficiency of cell replacement therapies in the retina and can be improved by MANF supplementation

(a) Representative images of cryosections, immunostained against GFP (green), from retinae of young (2-4mo) and old (24-30mo) mice, 14 days after subretinal delivery of Nrl-GFP photoreceptors. Nuclear staining with DAPI is shown in blue. (b) Quantification of the average number of GFP+ cells within the ONL of the retinae of young (2-4mo) and old (24-30mo) mice, 14 days after subretinal delivery of Nrl-GFP photoreceptors (n=10/age). (c) Representative images of cryosections, immunostained against GFP (green), from retinae of old (24-30mo) mice, 14 days after subretinal delivery of Nrl-GFP photoreceptors, with or without hrMANF supplementation. Nuclear staining with DAPI is shown in blue. (d) Quantification of the average number of GFP+ cells within the ONL of the retinae of old (24-30mo) mice, 14 days after subretinal delivery of Nrl-GFP photoreceptors, with or without hrMANF supplementation (n=3-6/condition). (e) Contingency analysis of all the animals in the study, grouped by integration efficiency, classified by the number of GFP+ cells in ONL ($p<0.0001$, Chi-square test). See also Supplemental Figure S3a. (f) Representative images of cryosections, immunostained against GFP (green), and CD68 (red) from retinae of young (2-4mo), old (24-30mo) mice, 14 days after subretinal delivery of Nrl-GFP photoreceptors with or without hrMANF supplementation. Nuclear staining with DAPI is shown in blue. For each column, three examples are shown, representing different grades of the phenotypes observed in the corresponding condition. Data are represented as average

± s.e.m. and each n represents one animal. p values in (b) and (d) are from two-tailed Student’s t-test.

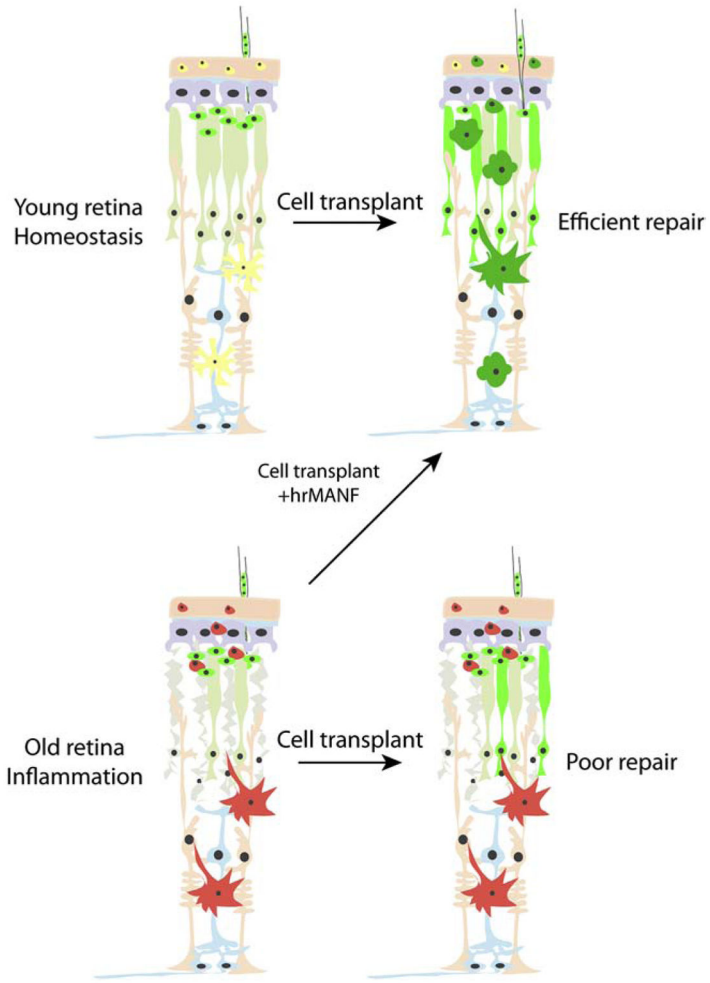

Figure 4: Model for and immune modulatory function of MANF in cell replacement therapies in the old retina.

Inflammation in the old retina constitutes a roadblock to the success of cell replacement therapies based of photoreceptor transplantation. Retinal inflammation is attenuated and cell integration improved when hrMANF is used as a co-adjuvant in the retinal transplants.